



Low-cost transfer between asteroids with distant orbits using multiple gravity assists

Hongwei Yang, Jingyang Li, Hexi Baoyin *

School of Aerospace Engineering, Tsinghua University, Beijing 100084, People's Republic of China

Received 2 February 2015; received in revised form 5 May 2015; accepted 6 May 2015

Available online 16 May 2015

Abstract

Low-cost transfer trajectories are significant to explore asteroids with distant orbits in a multiple targets' mission. Methods for designing these trajectories optimally are proposed. The sequence of gravity-assists is evaluated by the Tisserand graph. Then, an optimization method combining the particle swarm optimization (PSO) and the indirect method is used to optimize the low-thrust trajectories with gravity assists. The Bang–Bang control problem in the indirect method is overcome by a smooth technique. The whole transfer trajectories solving process by the shooting method is divided into several steps to overcome the difficulty and improve the efficiency. Numerical simulations are carried out for validating the proposed method.

© 2015 COSPAR. Published by Elsevier Ltd. All rights reserved.

Keywords: Asteroid; Gravity assist; Optimization; Low-thrust trajectory; Indirect method

1. Introduction

Both near-Earth asteroids and main-belt asteroids have attracted space agencies to carry out explorations. Several spacecrafts have explored these asteroids successfully, including NEAR Shoemaker (Dunham et al., 2002), Hayabusa-1 (Kawaguchi et al., 2008), Dawn (Russell et al., 2007), etc. The first two spacecrafts executed near-Earth asteroids' missions (Dunham et al., 2002; Kawaguchi et al., 2008) and the third one has finished rendezvousing the main-belt asteroid Vesta and is on its way to the Ceres (Russell et al., 2007). Several other future missions, such as MarcoPolo (Barucci et al., 2012), OSIRIS-REx (Lauretta and Team, 2012), Hayabusa 2 (Tsuda et al., 2013), etc., are proposed in the past years as well.

Near-Earth asteroids includes three types which are Apollo ($a \geq 1.0$ AU; $q \leq 1.0167$ AU), Aten ($a < 1.0$ AU; $q > 0.983$ AU) and Amor (1.0167 AU $< q \leq 1.3$ AU) (Morbidelli et al., 2002). Accessibility of exploring the near-Earth asteroids by direct transfer or using the Earth gravity assist has been studied and evaluated (Lau and Hulkower, 1987; Qiao et al., 2006). Different from the near-Earth asteroids, the orbits of the main-belt asteroids are distant to the Earth. These asteroids are usually divided into three groups according to the semimajor axis: the inner belt asteroids (2.1 AU $\leq a \leq 2.5$ AU), the middle belt asteroids (2.5 AU $< a \leq 3.0$ AU) and the outer belt asteroids ($a > 3.0$ AU) (Chen et al., 2014). Due to the orbits of the main-belt asteroids are distant, single and multiple gravity assists are studied to lower the mission cost and the accessibility is evaluated (Chen et al., 2014). Dual Mars gravity assists are shown to be the best via the analysis (Chen et al., 2014) and the dual Mars gravity assists are used twice in the sample return mission (Dankanich et al., 2010).

* Corresponding author.

E-mail addresses: yang.hw.thu@gmail.com (H. Yang), lijingyang10@mails.tsinghua.edu.cn (J. Li), baoyin@tsinghua.edu.cn (H. Baoyin).

Visiting multiple asteroids during one mission can reduce costs and increase the scientific results obviously (Olympio, 2011). Sears et al. and Morimoto et al. studied a mission of sampling return of multiple near-Earth asteroids (Sears et al., 2004; Morimoto et al., 2004). Olympio derived the transversality conditions for the optimal control of missions in which the multiple asteroids are visited by rendezvous or flyby (Olympio, 2011). Besides, visiting multiple asteroids is one of the main subjects of the global trajectory optimization competition (GTOC). In the recent 7th edition GTOC, a mission with multiple spacecrafts for visiting the asteroid belt is proposed (Casalino and Colasurdo, 2015). Actually, this is a multiple targets mission with several important features such as the simultaneous optimization of trajectories, cooperation between mothership and probes, etc. (Casalino and Colasurdo, 2015). Visiting near-Earth asteroids and main-belt asteroids in one mission can achieve scientific aims of studying both these two kinds of asteroids and lower the cost. One key part of designing such a mission is the transfer orbits between the near-Earth asteroids and main-belt asteroids.

Due to the orbits of a near-Earth asteroid and a main-belt asteroid is distant, the gravity assists are necessary to lower the cost significantly. Besides, the electric propulsion, which provides the low thrust, gives higher specific impulse and thus is more efficient compared with the traditional chemical propulsion (Jiang et al., 2012). Actually, the electric propulsion has already been used in the asteroid's mission for visiting the Itokawa (Kuninaka et al., 2007). So far, many works have been carried out for dealing with low-thrust trajectory design to outer planets combined with gravity assists (Armellin et al., 2010; Casalino et al., 1999; Jiang et al., 2012; McConaghy et al., 2003; Rasotto et al., 2013; Woo et al., 2006). McConaghy et al. (2003) proposed a two-step approach including the broad search and the parameter optimization. In the broad search, a simplified shape-based trajectory model is used and the best trajectories are selected by a heuristic cost function. Woo et al. (2006) employed the genetic algorithms and proposed automatic searching procedure. The methods developed by McConaghy et al. (2003) and Woo et al. (2006) are regarded as direct methods to deal with the optimal control problems. Different with their works, the fuel optimal low-thrust trajectories using multiple gravity assists are studied by the indirect method in this paper. In the indirect method, the optimal control problem is transformed into a boundary value problem with the help of the Pontryagin's Maximum theory and then solved by a shooting method (Rao, 2009). In the study of Casalino et al. (1999), the indirect method is used and both cases of free-height and minimum-height flybys are studied. Besides, the method proposed by Casalino et al. (1999) is able to deal with both cases of constant and variable exhaust velocity as well. Jiang et al. (2012) proposed a practical homotopic method which can be applied to solve the low thrust trajectories combined gravity assists. Both the studies of Casalino et al. (1999) and Jiang et al. (2012) dealt

with single gravity-assist problems. In the current paper, a multiple gravity-assist problem is to be studied. Rasotto et al. (2013) has proposed a method for dealing with the multiple gravity-assist problems using the multiple-shooting technique (Olympio, 2011). An intermediate point is selected within the arc between two planets to increase the robustness (Rasotto et al., 2013). Indeed, the multiple-shooting technique can greatly improve the convergence of solving the boundary value problems. But the number of the variables will increase quickly with number of the intermediate points as well. Besides, the boundary value problems may be hard to converge without proper guessed initial values when the number of the unknown variables is too large. Different with the approach of Rasotto et al. (2013), the method proposed in this paper is developed from the practical homotopic method (Jiang et al., 2012). The method proposed by Jiang et al. (2012) becomes very fast and effective in its solving process by involving two key techniques: (1) normalization of the initial costate vector; (2) switching detection. Actually, the practical homotopic method (Jiang et al., 2012) has shown its excellent efficiency for optimizing the low-thrust trajectories in the 5th edition GTOC (Jiang et al., 2014). The idea herein is to divide the whole low-thrust trajectories into several sub-trajectories and each contains only one gravity assist for the purpose of decreasing the number of the unknown variables. In this way, the practical homotopic method (Jiang et al., 2012) can be applied simply and effectively for optimizing each sub-trajectory. The whole low-thrust trajectories are then obtained by a three-step solving process. Although only the optimality of the sub-trajectories can be guaranteed by the method in the current paper, the proposed method is easy to converge and can be simply extended for low-thrust trajectory optimizations with more than three gravity assists.

As for the fuel optimal control problem, there always exists a Bang–Bang control problem which leads the convergence of the shooting process to be difficult (Bertrand and Epenoy, 2002). Bertrand and Epenoy (2002) proposed a smoothing technique in which an index homotopy is built to overcome this difficult. This method has been used and developed in many studies (Chen et al., 2014; Jiang et al., 2012; Olympio, 2011; Rasotto et al., 2013; Caillau et al., 2012; Yang and Baoyin, 2015). Specifically, Rasotto et al. (2013) proposed two kinds of smoothing approximations which are the exponential approximation and arctangent approximation. Besides, Rasotto et al. (2013) and Caillau et al. (2012) applied the smoothing technique to the optimal control problems with three-body dynamics; Yang and Baoyin (2015) dealt with the optimal control problems in irregular gravity fields. However, it is difficult to determine the switching points only by the smoothing technique. Switching time optimization methods are regarded as an efficient ways to determine the optimal Bang–Bang switching points (Lin et al., 2014; Loxton et al., 2014). In these methods, the key technique is the time-scaling transformation by which the existence of the partial derivatives of the

cost function can be guaranteed and the numerical integration becomes easier (Lin et al., 2014; Loxton et al., 2014). But the switching time optimization methods belong to direct methods. Alternatively, the switching detection combined with the smoothing technique, which belongs to indirect methods, shows its advantages in determining the switching points accurately and efficiently as well (Jiang et al., 2012). In this paper, the method proposed by Jiang et al. (2012) is used. Moreover, the magnitude of the low thrust is assumed to be varying with the distance to the sun other than being constant in the current study. Hence, the key equations of the switching detection (Jiang et al., 2012) will be derived for the new case.

Moreover, this paper focuses on the specific case of designing low thrust trajectories between a near-Earth asteroid and a main-belt asteroid using gravity assists which is not considered in these previous studies (Armellin et al., 2010; Casalino et al., 1999; Jiang et al., 2012; McConaghy et al., 2003; Rasotto et al., 2013; Woo et al., 2006). Although the low thrust trajectories from the Earth to the main-belt asteroids with gravity assists have been studied in the work of Chen et al. (2014), the spacecraft is started from a near-Earth asteroid rather than the Earth in this paper. Hence, the selected sequence of the gravity assist will be different from the one in the work of Chen et al. (2014). Based on the results of Chen et al. (2014), the best sequence of the gravity assist for transfers between a near-Earth asteroid and a main-belt asteroid is further analyzed and determined by the Tisserand graph (Strange and Longuski, 2002). With the determined gravity-assist sequence, an optimization method combining the PSO method and the indirect method is proposed to optimize the transfer trajectories. It is expected that the gravity-assist analysis and the proposed optimization method can be useful for the orbit design of future multiple-asteroid explorations of visiting both near-Earth asteroids and main-belt asteroids.

2. Problem statement and basic analysis

2.1. Problem statement

A spacecraft propelled by low thrusters is assumed to have finished a rendezvous mission with a near-Earth asteroid at the initial time t_0 . The initial position vector \mathbf{r}_0 and velocity vector \mathbf{v}_0 are assumed to be the same as the near-Earth asteroid. Then, the spacecraft starts to execute an interplanetary transfer by the low thrust. The dynamical equation of the low-thrust propelled spacecraft in the heliocentric ecliptic reference frame, when only the spherical gravity of the sun is considered beside the low thrust for preliminary designs, is (Jiang et al., 2012)

$$\dot{\mathbf{r}} = \mathbf{v}, \quad \dot{\mathbf{v}} = -\frac{\mu}{r^3}\mathbf{r} + \frac{T_{\max}u}{m}\boldsymbol{\alpha}, \quad \dot{m} = -\frac{T_{\max}u}{I_{sp}g_0} \quad (1)$$

where \mathbf{r} and \mathbf{v} are the position and velocity vectors, respectively, μ is the gravitational constant of the sun, u is the

engine thrust ratio, m is the mass of the spacecraft, I_{sp} is the thruster specific impulse, $g_0 = 9.80665 \text{ m/s}^2$ is the standard acceleration of the gravity at sea level, and T_{\max} is the instantaneous maximal thrust magnitude and is assumed to be depended on the distance r from the sun:

$$T_{\max} = T_0/r^2 \quad (2)$$

Here, T_0 is maximal magnitude of the thrust at the distance 1 astronomical unit (AU) to the sun. At terminal time t_f , the spacecraft is assumed to rendezvous a main-belt asteroid, i.e., its terminal position and velocity vectors, \mathbf{r}_f and \mathbf{v}_f , are the same as the asteroid.

To lower the cost of the interplanetary transfer, gravity assists are assumed to be used. In this paper, the impulsive model of gravity assists which has been employed for preliminary trajectories' design or analysis (Chen et al., 2014; Jiang et al., 2012; Sims and Flanagan, 1997) is used. In this model, the position spacecraft is assumed to be the same as the gravity-assist planet at the instantaneous gravity-assist time t_{GA} :

$$\mathbf{r}(t_{GA}) - \mathbf{r}_P(t_{GA}) = 0 \quad (3)$$

The change of the velocity is shown in Fig. 1 and the following equations are satisfied (Jiang et al., 2012):

$$\mathbf{v}^- = \mathbf{v}_P + \mathbf{v}_\infty^- \quad (4)$$

$$\mathbf{v}^+ = \mathbf{v}_P + \mathbf{v}_\infty^+ \quad (5)$$

$$\|\mathbf{v}_\infty^-\| = \|\mathbf{v}_\infty^+\| = v_\infty \quad (6)$$

$$\cos \delta = \frac{\mathbf{v}_\infty^- \cdot \mathbf{v}_\infty^+}{v_\infty^2}, \quad \delta \leq \delta_{\max} \quad (7)$$

where “-” and “+” denote the instantaneous time before and after the t_{GA} , \mathbf{v}_P is velocity vector of the gravity-assist planet, \mathbf{v}_∞^- and \mathbf{v}_∞^+ are inbound or outbound excess velocity vectors, respectively, and δ is the turn angle. The maximal turn angle δ_{\max} is determined by (Jiang et al., 2012)

$$\sin \frac{\delta_{\max}}{2} = \frac{1}{1 + r_{\min}^p v_\infty^2 / \mu_P} \quad (8)$$

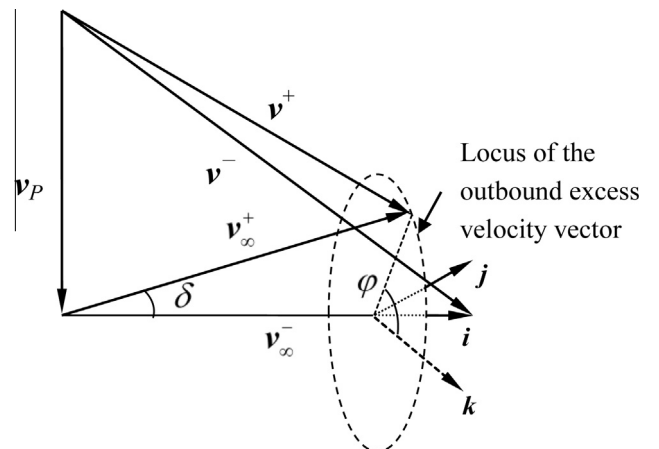


Fig. 1. Illustration of the gravity-assist impulsive model.

where μ_P is gravitational constant of the planet and r_{\min}^p is the minimum flyby radius.

As shown in Fig. 1, the locus of the outbound excess velocity vector is a circular which is perpendicular to the vector of the inbound excess velocity when the turn angle is specified. Define a gravity-assist frame $o-ijk$, where

$$\mathbf{i} = \frac{\mathbf{v}_{\infty}^-}{\|\mathbf{v}_{\infty}^-\|}, \quad \mathbf{k} = \frac{\mathbf{v}_P \times \mathbf{v}_{\infty}^-}{\|\mathbf{v}_P \times \mathbf{v}_{\infty}^-\|}, \quad \mathbf{j} = \mathbf{k} \times \mathbf{i} \quad (9)$$

Then, the following equation can be obtained:

$$\mathbf{v}_{\infty}^+ = v_{\infty} (\cos \delta \mathbf{i} + \sin \delta \sin \phi \mathbf{j} + \sin \delta \cos \phi \mathbf{k}) \quad (10)$$

The impulse provided by the gravity assist is

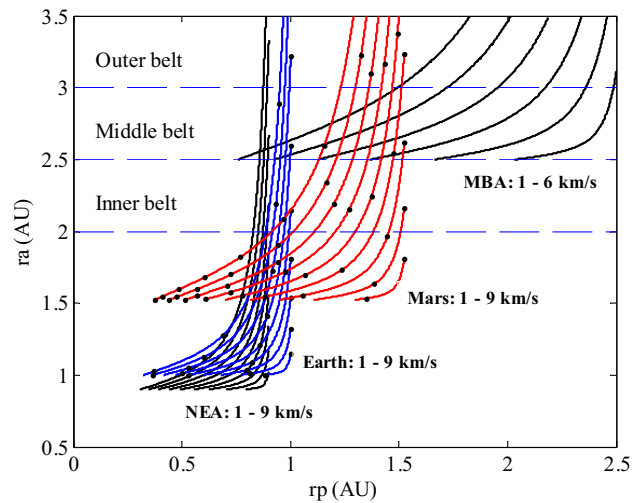
$$\Delta \mathbf{v}_{GA} = \mathbf{v}^+ - \mathbf{v}^- \quad (11)$$

2.2. Gravity-assist sequence analysis

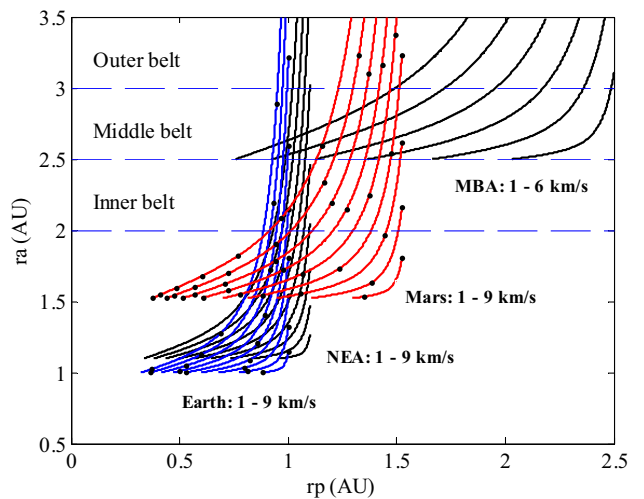
The Tisserand graph is an analytical method developed by Strange and Longuski (2002) for analyzing sequences of gravity assists. This method has been used to select gravity-assist planets for rendezvousing main-belt asteroids by a spacecraft launched from the Earth (Chen et al., 2014). In the study of Chen et al. (2014), the dual Mars gravity assist is shown to be most effective and the Venus is inefficient for main-belt asteroid missions. Different with their study, the spacecraft is launched from a near-Earth asteroid rather than the Earth. The Venus is ignored in the current study as well due to the assumption that only the near-Earth asteroids with orbits close to the Earth are considered in this paper. The R_a-R_p plot (i.e. one form of the Tisserand graph) (Chen et al., 2014), in which the horizontal axis and ordinate axis denote the periapsis R_p and apoapsis R_a of the transfer orbit connecting the corresponding celestial body, respectively, is used herein for gravity-assist sequence analysis.

In the graphical method, the orbits of all celestial bodies are assumed to be circular and coplanar (Strange and Longuski, 2002). Specially, these celestial bodies include the Earth, Mars, near-Earth asteroids and main-belt asteroids in the current study. Based on the previous study (Chen et al., 2014), the Mars gravity assist should be effective due to the orbit of the near-earth asteroid is close to the Earth. Indeed, the effect of the Mars gravity assist will be demonstrated by the R_a-R_p plots. To further study the effectiveness of the Earth gravity assist when the spacecraft is launched from a near-Earth asteroid, both cases for semimajor axis a of the near-Earth asteroid being larger or smaller than the Earth will be checked. Herein, the semimajor axis of the near-Earth asteroid is chosen to be 0.9 AU or 1.1 AU. Besides, the semimajor axis of the target main-belt asteroid has no direct impact on the effectiveness of the Earth gravity assist because the Mars gravity assist is suggested (Chen et al., 2014) before arriving at the main belt. Hence, the semimajor axis of the main-belt asteroid herein is arbitrarily chosen to be 2.5 AU in the graphical analysis.

The R_a-R_p plots for the near-Earth asteroid, Earth, Mars and main-belt asteroid are shown in Fig. 2(a) and (b). The abbreviations NEA and MBA represent near-Earth asteroid and main-belt asteroid in this figure as well as the figures and tables below. In the R_a-R_p plots, the curves represent v_{∞} contours of the planets or asteroids. The v_{∞} is defined as the velocity difference between the transfer orbits and the orbit of a celestial body. The contours are obtained as follows. Denote the angle between the v_{∞} and the velocity of each planets or asteroids as α . With a given α and the magnitude of the v_{∞} , the periapsis and apoapsis of the transfer orbit can be determined. By varying α while maintaining the magnitude of the v_{∞} , a series of R_a and R_p for a v_{∞} contour can be obtained. In this study, the α is equal to 0° at the upper bound of each contour and it increases to 180° at the lower bound of the contour. Besides, the value of the contours for each celestial body increases from right to left with the interval of



(a) Semimajor axis of the NEA is 0.9 AU



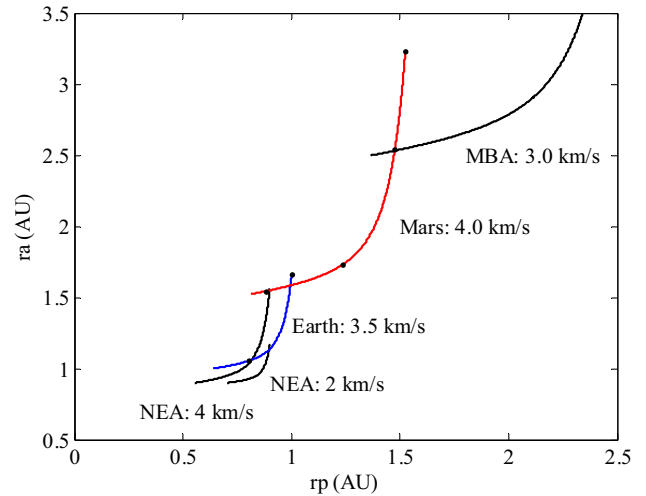
(b) Semimajor axis of the NEA is 1.1 AU

Fig. 2. R_a-R_p plots for NEA, Earth, Mars and MBA.

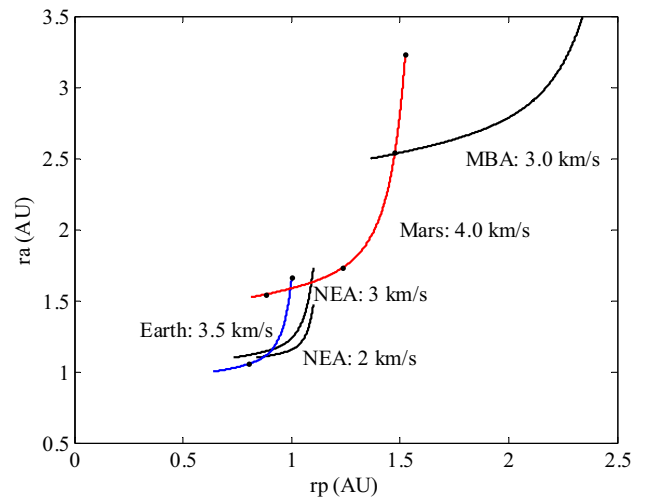
1 km/s. For example, there are nine v_∞ contours for the Earth and the value of these contours is 1–9 km/s from right to left. Moreover, in order to find a transfer orbit between two celestial bodies, there should be an intersection of the v_∞ contours of these two celestial bodies. The angle α can be changed by gravity assists. Hence, one intersection can be shifted to another intersection on the same contour by the planet’s gravity assists. However, the capacity of the gravity assist for changing α is limited. The capacity of one gravity assist is reflected by the tick markers on the planets’ contours. Specifically, there can be a shift on a curve but the shift cannot pass more than one tick marker by one gravity assist. More detail information for the R_a – R_p plots can be found in the works of Chen et al. (2014) and Strange and Longuski (2002).

As shown in Fig. 2, the v_∞ contours of the Mars can connect the 3 km/s contour of the main-belt asteroid while the v_∞ contours of the Earth and near-Earth asteroid intercept the contour of the main-belt asteroid with value of 5 km/s at least. Hence, the braking impulse can be greatly decreased with the help of the Mars gravity assist. Besides, only the v_∞ contour of the Earth or the near-Earth asteroid with high value can connect the contour of the main-belt asteroid without the Mars gravity assist which means the launch velocity should be large. Hence, the Mars gravity assist is necessary. Minimum total impulse cases of either using Earth gravity assist or not are selected from Fig. 2 and plotted in Fig. 3 to illustrate the effectiveness of the Earth gravity assist. For both cases in Fig. 3, it can be founded that the launch impulse from the near-Earth asteroid can be reduced with the help of the Earth gravity assist. In Fig. 3(a), the launch impulse is 2 km/s with the Earth gravity assist while it is 4 km/s without the Earth gravity assist; In Fig. 3(b), the launch impulse is 2 km/s with the Earth gravity assist while it is 3 km/s without the Earth gravity assist. Hence, the Earth gravity assist is necessary for reducing the total impulse. Besides, there is a potential application that is to return the sample collected from the near-Earth asteroid during the Earth gravity assist. Moreover, dual Mars gravity assists are required according to the tick markers on the v_∞ contour of the Mars. This phenomenon consists with the result of the work of Chen et al. (2014).

According to Fig. 3 and the analysis above, the best gravity assist sequence is Earth–Mars–Mars gravity assist (EMMGA). This sequence will be used in next analysis and simulations. Note that all trajectories corresponding to the contours in Fig. 3 are ballistic not low-thrust propelled and the appropriate phases are assumed for rendezvous and gravity assists. Actually, the impulsive maneuver approximation is one of most effective methods used in preliminary analysis and global searching for low thrust trajectories designing (Olympio, 2011; Sims and Flanagan, 1997). Besides, appropriate phases can be found with the assumption that the allowed range of the launch date is large enough.



(a) Semiaxis of the NEA is 0.9 AU



(b) Semiaxis of the NEA is 0.9 AU

Fig. 3. Illustration of the effectiveness of the Earth gravity assist.

3. Optimal delta-V searching

The overall process of the optimization method in the current study for obtaining the low-thrust trajectories is as follows. Firstly, the impulsive maneuver approximation (Sims and Flanagan, 1997) is used for searching global optimal delta-V trajectories. The PSO method is chosen as the global optimization method to design the event dates and the whole delta-V of impulsive maneuvers is obtained by the patched conic method. Secondly, an indirect method is used to optimize low-thrust trajectories. In the indirect method, the event dates obtained in the previous step, including launch time, gravity assist time and braking time, are used as guessed values.

The patched conic method is illustrated in Fig. 4(a). The lambert method is used directly to construct the transfer trajectories between every two celestial bodies except for the trajectory connecting the consecutive Mars gravity assists. The reason for not solving this special case directly

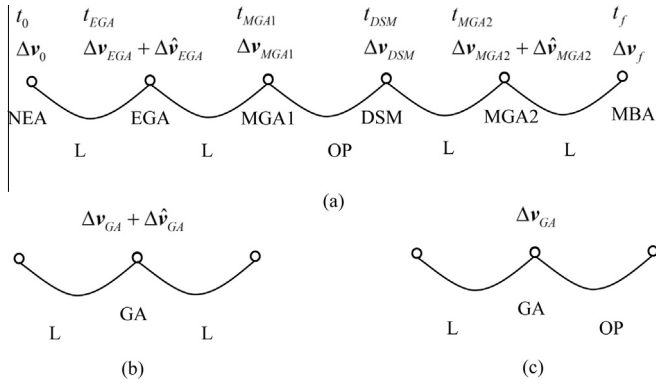


Fig. 4. Illustration of the patched conic method.

by the Lambert method is as follows. The consecutive gravity assists are ideal resonant gravity assists if no deep space maneuver (DSM) is carried out. In this case, the trajectory is a 360° transfer and the Lambert method cannot work well to determine the trajectory. Followed the way of [Chen et al. \(2014\)](#), a DSM is assumed between the two Mars gravity assists. Actually, the DSM is also essential in the V_∞ leveraging technique to improve the effectiveness of the consecutive gravity assists provided by the same Planet ([Sims et al., 1997](#)). Hence, the total delta-V may be decreased with the help of the DSM. Moreover, it should be noted that the magnitude of the DSM can be very small in the optimized result.

The time variables in [Fig. 4\(a\)](#) are as follows: the initial time t_0 , the Earth gravity assist (EGA) time t_{EGA} , the first Mars gravity assist (MGA1) time t_{MGA1} , the DSM time t_{DSM} , the second Mars gravity assist (MGA2) time t_{MGA2} , and the terminal time t_f . Five impulses are assumed to be provided by the thrusters. $\Delta \mathbf{v}_0$ is the launch impulse, $\Delta \mathbf{v}_f$ is terminal brake impulse, $\Delta \hat{\mathbf{v}}_{EGA}$ and $\Delta \hat{\mathbf{v}}_{MGA2}$ are impulses executed instantaneously after the gravity assists, and $\Delta \mathbf{v}_{DSM}$ is the impulse for the DSM. Moreover, $\Delta \mathbf{v}_{EGA}$, $\Delta \mathbf{v}_{MGA1}$ and $\Delta \mathbf{v}_{MGA2}$ are impulses provided by the Earth or Mars.

In [Fig. 4](#), L means solving a transfer leg by the Lambert solution and OP means solving a transfer leg by the orbit propagation. Hence, there are two kinds of gravity assist as shown in [Fig. 4\(b\)](#) and (c). This is because the target position of the spacecraft when the DSM is executed cannot be obtained only by the t_{DSM} . At other five time, the target position is equal the position of the asteroids or planets. The relationships of the velocity after and before the gravity assist, \mathbf{v}_{out} and \mathbf{v}_{in} , in [Fig. 4\(b\)](#) and (c) are

$$\mathbf{v}_{out} = \mathbf{v}_{in} + \Delta \mathbf{v}_{GA} + \Delta \hat{\mathbf{v}}_{GA} \quad (12)$$

$$\mathbf{v}_{out} = \mathbf{v}_{in} + \Delta \mathbf{v}_{GA} \quad (13)$$

$\Delta \mathbf{v}_{GA}$ is chosen to minimize the magnitude of $\Delta \hat{\mathbf{v}}_{GA}$ in Eq. (12) while it is determined by the two gravity-assist angles δ and φ as shown in [Fig. 1](#).

The optimal delta-V index can be chosen as

$$J = \|\Delta \mathbf{v}_0\| + \|\Delta \hat{\mathbf{v}}_{EGA}\| + \|\Delta \mathbf{v}_{DSM}\| + \|\Delta \hat{\mathbf{v}}_{MGA2}\| + \|\Delta \mathbf{v}_f\| \quad (14)$$

where $\|\cdot\|$ denotes second norm of the vector.

To solve the optimal delta-V problem, the particle swarm optimization (PSO) method ([Pontani and Conway, 2010](#); [Kennedy, 2010](#)) is used. The optimal variables are x_i ($i = 1, \dots, 8$) $\in [0, 1]$. Then, the following variables required for patched conic method are expressed by these optimal variables:

$$\begin{aligned} t_0 &= t_{0s} + (t_{0f} - t_{0s})x_1 \\ t_{EGA} &= t_0 + dt_{\max}x_2 \\ t_{MGA1} &= t_{EGA} + (dt_{\max} - (t_{EGA} - t_0))x_3 \\ t_{DSM} &= t_{MGA1} + (dt_{\max} - (t_{MGA1} - t_0))x_4 \\ t_{MGA2} &= t_{DSM} + (dt_{\max} - (t_{DSM} - t_0))x_5 \\ t_f &= t_{MGA2} + (dt_{\max} - (t_{MGA2} - t_0))x_6 \\ \varphi_{MGA1} &= 2\pi x_7 \\ \delta_{MGA1} &= \delta_{\max}x_8 \end{aligned} \quad (15)$$

Once the variables above are determined, the ballistic trajectories can be then obtained. And the optimized time variables are to be further used in the following low-thrust trajectory design. Besides, the state variables of impulsive transfers at each t_{GA}^+ and t_{GA}^- will be employed as temporary boundary-value conditions.

4. Low-thrust trajectory optimization

4.1. Optimal control for variable-thrust trajectory

To minimize the fuel consumption, the following index is chosen:

$$J = \lambda_0 \int_{t_0}^{t_f} \frac{T_{\max} u}{I_{sp} g_0} dt \quad (16)$$

where λ_0 is positive constant. According to the Pontryagin's Maximal Theory, the following Hamiltonian H is built ([Jiang et al., 2012](#); [Zeng et al., 2014](#)):

$$H = \lambda_r \cdot \mathbf{v} + \lambda_v \cdot \left(-\frac{\mu}{r^3} \mathbf{r} + \frac{T_{\max} u \boldsymbol{\alpha}}{m} \right) - \lambda_m \frac{T_{\max} u}{I_{sp} g_0} + \lambda_0 \frac{T_{\max} u}{I_{sp} g_0} \quad (17)$$

where λ_r , λ_v and λ_m are co-state variables.

Based on the Euler-Lagrange conditions, the differential equations for the co-state variables can be obtained:

$$\begin{aligned} \dot{\lambda}_r &= \frac{\mu}{r^3} \lambda_v - \frac{3\mu \mathbf{r} \cdot \lambda_v}{r^5} \mathbf{r} + \lambda_v \cdot \frac{2T_0 u \boldsymbol{\alpha}}{r^4} \mathbf{r} - 2(\lambda_m - \lambda_0) \frac{T_0 u}{I_{sp} g_0 r^4} \mathbf{r} \\ \dot{\lambda}_v &= -\lambda_r \\ \dot{\lambda}_m &= \lambda_v \cdot \frac{T_{\max} u \boldsymbol{\alpha}}{m^2} \end{aligned} \quad (18)$$

The optimal thrust direction and magnitude should be chosen to guarantee that the Hamiltonian is minimized. Hence, the optimal thrust direction and magnitude can be obtained as follows:

$$\alpha^* = -\frac{\lambda_v}{\|\lambda_v\|} \tag{19}$$

$$u^* = \begin{cases} 1, & \rho < 0 \\ 0, & \rho > 0 \\ [0, 1], & \rho = 0 \end{cases} \tag{20}$$

where the expression of the switching function ρ is

$$\rho = 1 - \frac{I_{sp}g_0\|\lambda_v\|}{\lambda_0 m} - \frac{\lambda_m}{\lambda_0} \tag{21}$$

So far, the optimal control expressions have been derived as Eqs. (19) and (20).

4.2. Multiple-point-boundary-value problem

The ordinary differential equations for this optimal control problem are Eqs. (1) and (18) which are

$$\dot{x} = f(x, U, t) = \begin{cases} \dot{\mathbf{r}} = \mathbf{v} \\ \dot{\mathbf{v}} = -\frac{\mu}{r^3}\mathbf{r} + \frac{T_{\max}u}{m}\alpha \\ \dot{m} = -\frac{T_{\max}u}{I_{sp}g_0} \\ \dot{\lambda}_r = \frac{\mu}{r^3}\lambda_v - \frac{3\mu r\lambda_v}{r^5}\mathbf{r} + \lambda_v \cdot \frac{2T_0u\mathbf{z}}{r^4}\mathbf{r} - 2(\lambda_m - \lambda_0)\frac{T_0u}{I_{sp}g_0r^4}\mathbf{r} \\ \dot{\lambda}_v = -\lambda_r \\ \dot{\lambda}_m = \lambda_v \cdot \frac{T_{\max}u\mathbf{z}}{m^2} \end{cases} \tag{22}$$

In this paper, the initial and terminal time are assumed to be fixed to the optimized values in Eq. (15). According to the assumptions in Section 2.1, the initial and terminal constraints are

$$\begin{aligned} \mathbf{r}(t_0) - \mathbf{r}_{NEA}(t_0) &= 0 \\ \mathbf{v}(t_0) - \mathbf{v}_{NEA}(t_0) &= 0 \\ m(t_0) - m_0 &= 0 \end{aligned} \tag{23}$$

$$\begin{aligned} \mathbf{r}(t_f) - \mathbf{r}_{MBA}(t_f) &= 0 \\ \mathbf{v}(t_f) - \mathbf{v}_{MBA}(t_f) &= 0 \end{aligned} \tag{24}$$

respectively. A terminal transversality condition can be obtained due to no mass constraint in Eq. (24):

$$\lambda_m(t_f) = 0 \tag{25}$$

The intermediate gravity assists are regarded as interior point constraints and the intermediate dates are assumed to be variable. For each gravity assist, there are a four dimensional equality constraint and a one dimensional inequality constraint (Jiang et al., 2012):

$$\begin{aligned} \psi &= \begin{bmatrix} \mathbf{r}(t_{GA}) - \mathbf{r}_P(t_{GA}) \\ v_{\infty}^- - v_{\infty}^+ \end{bmatrix} = 0 \\ \sigma &= 1 - r_p/r_{\min} \leq 0 \end{aligned} \tag{26}$$

where r_p is flyby radius and r_{\min} is minimum flyby radius. In the works of Jiang et al. (2012), the transversality conditions for a gravity assist have been derived as

$$\begin{aligned} \lambda_r(t_{GA}^+) &= \lambda_r(t_{GA}^-) - \chi_{1\sim 3} \\ \lambda_v(t_{GA}^+) &= \chi_4 \hat{\mathbf{i}}^+ + \frac{1}{r_{\min}} \kappa \mathbf{B} \\ \lambda_v(t_{GA}^-) - \chi_4 \hat{\mathbf{i}}^- + \frac{1}{r_{\min}} \kappa \mathbf{A} &= 0 \\ H(t_{GA}^-) - H(t_{GA}^+) - \chi_{1\sim 3} \cdot \mathbf{v}_P(t_{GA}) \\ &+ \chi_4(\hat{\mathbf{i}}^+ - \hat{\mathbf{i}}^-) \cdot \mathbf{a}_P(t_{GA}) - \frac{1}{r_{\min}} \kappa C = 0 \end{aligned} \tag{27}$$

Detail information for \mathbf{A} , \mathbf{B} , \mathbf{C} and \mathbf{i} can be found in their work. Besides, a complementary slackness condition should be added due to the inequality constraint, which is (Jiang et al., 2012)

$$\kappa \cdot \sigma = 0, \quad \kappa \geq 0 \tag{28}$$

The unknowns for this multiple-point-boundary-value problem (MPBVP) are 34 dimensional, which are

$$\begin{aligned} \bar{X} &= (\lambda_0; \lambda_{r0}; \lambda_{v0}; \lambda_{m0}; t_{EGA}; t_{MGA1}; t_{MGA2}; \chi_{1-4}^{EGA}; \chi_{1-4}^{MGA1}; \\ &\times \chi_{1-4}^{MGA2}; \kappa^{EGA}; \kappa^{MGA1}; \kappa^{MGA2}; \Delta \mathbf{v}_{EGA}; \Delta \mathbf{v}_{MGA1}; \Delta \mathbf{v}_{MGA2}) \end{aligned} \tag{29}$$

The boundary conditions for the shooting function $\Phi(\bar{X})$ includes Eqs. (23)–(26) and (28) last two conditions in Eq. (27) and a normalization condition (Jiang et al., 2012)

$$\sqrt{\lambda_0^2 + \chi_{1-4}^{EGA} \cdot \chi_{1-4}^{EGA} + \kappa^{EGA} \cdot \kappa^{EGA} + \dots} = 1 \tag{30}$$

4.3. Solving method

Eq. (20) indicates the optimal control is a Bang–Bang control which leads to the convergence of solving the shooting function being very difficult (Bertrand and Epenoy, 2002). A smoothing technique, in which a homotopy is built, has been proposed to overcome this difficulty. In this paper, the following homotopy is used:

$$J = \lambda_0 \frac{T_{\max}}{I_{sp}g_0} \int_{t_0}^{t_f} [u - \varepsilon u(1 - u)] dt \tag{31}$$

The optimal control law is continuous provided ε is not equal to zero. The parameter ε establishes the connection between the energy optimal criteria ($\varepsilon = 1$) and fuel optimal criteria ($\varepsilon = 0$) (Jiang et al., 2012; Yang and Baoyin, 2015). The detail homotopic process can found in the work of Jiang et al. (2012). In their work, a switching function detection technique is used to determine the switching point accurately. The key issue is to calculate the switching function at $(k + 1)$ th step using the information at k th step (Yang and Baoyin, 2015):

$$\rho_{k+1} = \rho_k + \dot{\rho}_k h + \frac{1}{2} \ddot{\rho}_k h^2 \tag{32}$$

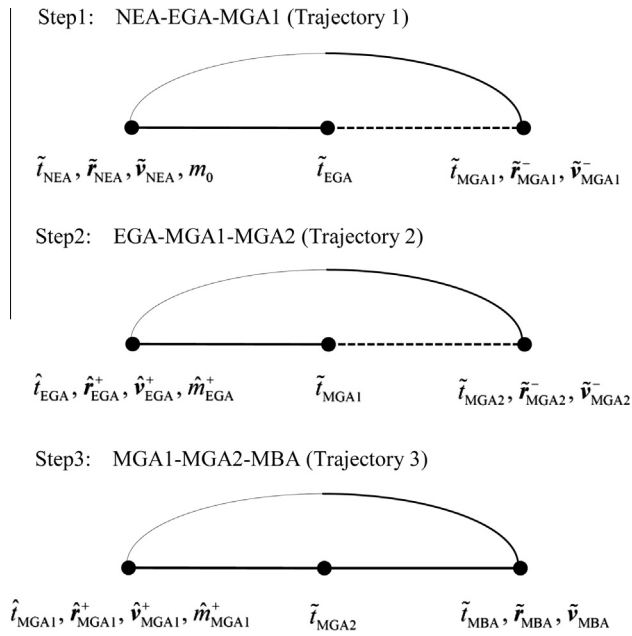


Fig. 5. Three-step solving process.

As for the problem that the thrust magnitude is not constant, the first and second orders of the switching function are

$$\dot{\rho} = \frac{I_{sp}g_0 \lambda_r \cdot \lambda_v}{\lambda_0 m \|\lambda_v\|} \quad (33)$$

$$\ddot{\rho} = \frac{I_{sp}g_0}{\lambda_0 m \|\lambda_v\|} \left(\dot{\lambda}_v \cdot \lambda_r + \dot{\lambda}_r \cdot \lambda_v - \frac{\dot{m} \lambda_r \cdot \lambda_v}{m} + \frac{(\lambda_r \cdot \lambda_v)^2}{\|\lambda_v\|^2} \right) \quad (34)$$

The shooting function of this MPBVP has 35 unknowns totally. In the work of Jiang et al. (2012), it has been shown the proposed method is very efficient for solving the optimal trajectory which contains one gravity assist. However, the good convergence cannot be guaranteed by applying the previous method (Jiang et al., 2012) directly due to the larger number of unknowns. To deal with this problem, the low thrust trajectories using triple gravity assists are divided into three trajectories as shown in Fig. 5 and then solved by a three-step method.

In Fig. 5, a symbol with “~” denotes that the value of the variable is obtained by the PSO method in Section 3. A symbol with “^” denotes the value of the variable is obtained from the optimal low thrust trajectory in the previous step. The detail process of the three-step method is as follows. In the method shown in Fig. 5, each step solves one optimal low thrust trajectory containing a single

interior point (i.e. only one gravity assist). For example, the only interior point constraints in step 1 are Eqs. (26)–(28) associated with the Earth gravity assist. As for the trajectory 1, the initial time, terminal time and the guessed Earth gravity assist are the results from the PSO searching. The initial and terminal boundary conditions are chosen so that the state variables (position, velocity and mass) are equal to the ones which are obtained from the PSO searching at the launch time and instantaneous time before the first Mars gravity assist. After the optimal low thrust trajectory 1 has been obtained, the time and state variables (position, velocity and mass) at the Earth gravity assist are updated using the results of the optimized trajectory 1. Then, these updated values are employed to be the initial conditions for the trajectory 2. Analogous to the trajectory 1, the optimal trajectory 2 is obtained and the state variables at the first Mars gravity assist are then used for solving the trajectory 3. Once the optimal trajectory 3 has been solved, the whole low-thrust transfer using triple gravity assists can be obtained by patching the first half of the trajectory 1 and trajectory 2, and the whole trajectory 3. Actually, the patched trajectories are represented by solid lines while the non-patched trajectories are represented by dash lines in Fig. 5. It should also be noted that the initial boundary condition of the trajectory 1 and the terminal boundary condition of the trajectory 3 consist with the Eqs. (23) and (24) due to the assumptions in Section 2.1. Importantly, the optimization method for the low thrust trajectories in each step is the practical homotopic method proposed by Jiang et al. (2012) with updated dynamical Eq. (22) and the condition of the accurate detection of the switching points 32–34.

5. Simulations and results

The near-Earth asteroid is assumed to be 2009 DB43 and the main-belt asteroid is assumed to be van Albada. The orbital elements of the asteroids and planets are listed in Table 1. In the optimal delta-V searching, the launch date is assumed in 59,140–59,500 MJD and maximum of the flight time is assumed to be 2500 days.

Once the optimal delta-V transfer has been obtained by the PSO method, the following parameters will be used for optimizing the low-thrust trajectories. These parameters are guessed intermediate time and terminal state variables in Table 2.

Then, the three-step method process is carried out to obtain the low-thrust trajectories. Here, the low thrust magnitude at 1 AU is assumed to be 0.3 N and the thruster

Table 1
Orbital elements of the asteroids and planets.

Item	Epoch (MJD)	<i>a</i> (AU)	<i>e</i>	<i>i</i> (deg)	Ω (deg)	ω (deg)	<i>M</i> (deg)
Earth	54,000	1.0008404	0.016507	0.001218	1.770191	98.504893	260.350296
Mars	54,000	1.523677	0.0934357	1.849299	49.538448	286.561587	226.112109
2009 DB43	56,000	1.102335	0.172238	0.934297	43.778992	38.52093	283.364464
van Albada	56,000	2.240859	0.204204	7.195726	355.140792	324.150502	144.442036

Table 2
Parameters for the three-step solving process.

Item	Initial time (MJD)	Terminal time (MJD)	Guessed intermediate time (MJD)	Initial state variable (AU, AU/year, kg)	Terminal state variable (AU, AU/year)
NEA-EGA-MGA1	59448.923	60288.786	59871.765	0.538775	-0.586627
				0.755812	-1.389018
				0.002820	-0.014693
				-5.983291	4.784104
				3.665783	-0.718020
				0.110674	-0.028847
EGA-MGA1-MGA2	59882.238	60975.756	60288.786	1500	
				0.813596	-0.586627
				0.522950	-1.389018
				-0.001022	-0.014693
				-3.472516	5.045071
				6.255490	-0.917749
MGA1-MGA2-MBA	60296.657	61592.624	60975.756	0.091765	0.395806
				1467.692572	
				-0.479378	-0.873644
				-1.418904	2.444605
				-0.014431	-0.111541
				5.256989	-3.299789
				-0.444256	-1.357957
				0.485681	-0.193087
1435.269452					

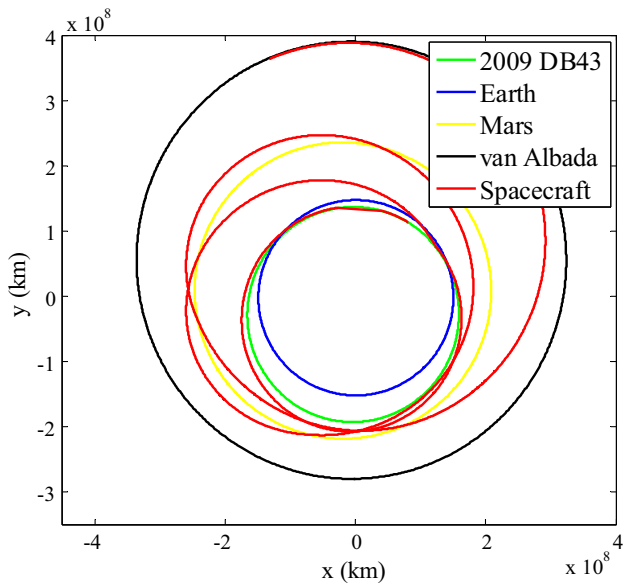


Fig. 6. The transfer trajectory projection in the ecliptic plane.

specific impulse is assumed to be 1500 s. The parameters for the three-step solving process are listed in Table 2.

Once the three sub-trajectories have been optimized, the whole low-cost transfer is then obtained via patching these three optimal sub-trajectories as illustrated in Fig. 5. The low-cost trajectories are shown in Fig. 6 and the low-thrust profile is shown in Fig. 7.

All computations above are coded in FORTRAN language and then executed on a personal laptop with an Intel Core i5-4210 CPU and 4 GB RAM. In the PSO procedure, the maximum iterations are set to be 5000. The

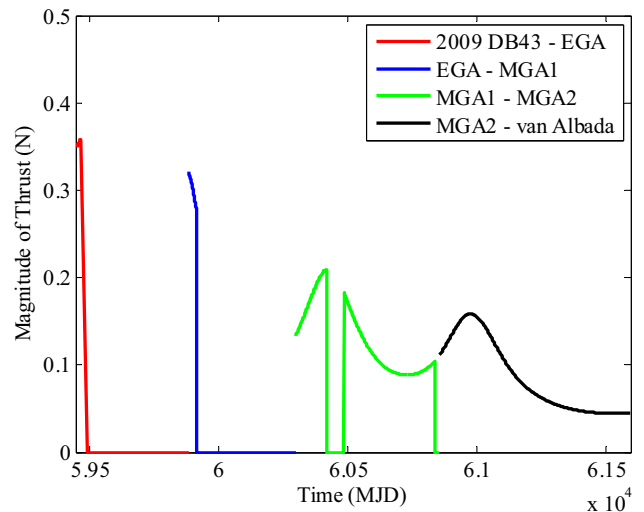


Fig. 7. Control profile of the low-thrust in a triple-GA sample trajectory.

PSO procedure is repeatedly executed 5 times and the best result is chosen. These computations cost about 100 s. In the three-step solving process, the computation time for obtaining initial values of the energy optimal case in each step is 0.140, 0.172 and 0.203 s, respectively. And the computation time cost for obtaining the fuel optimal solutions via the homotopic processes is 19.875, 6.568 and 1.295 s, respectively. The computation time is short even for the slowest step. Besides, the procedure of the three-step solving method is further tested several times for this example and the results show that the convergence can be guaranteed. Actually, the first author, as a member of the team of Tsinghua University, has participated in the GTOC7 and 4th edition Chinese trajectory optimization

competition (CTOC4). In the GTOC7, a similar homotopic procedure was used. Our team's primary index is 32 and only three teams (JPL, ACT/ESA-ISAS and University of Texas at Austin) got higher primary index, 36, 35 and 35, than us.¹ Moreover, a similar three-step solving method was used in CTOC4 of which the background is to visit different types of small bodies (Gao, 2012). In our submitted solution, one important part of the designed mission is the transfer from 2010 JR34 (a near-Earth asteroid) to Universitas (a main-belt asteroid) via EMMGA which is very similar to the example in this paper. Our team ranked the second with a score of 118 among the 23 registered teams and National University of Defense Technology ranked the first with a score of 120 (Gao, 2012). Because the result of the National University of Defense Technology is about a mission of visiting comets, our result is the best one for visiting both near-Earth asteroids and main-belt asteroids in CTOC4 which shows the good performance of our proposed method.

6. Conclusion

The low-cost transfer between a near-Earth asteroid and a main-belt asteroid using low thrust propulsion and multiple gravity assists has been studied. Based on the result of Chen et al. (2014), the gravity-assist sequence is further studied via the Tisserand graph and the sequence EMMGA is found to be the best. The PSO method and indirect method are combined to optimize low-thrust trajectories. Firstly, the optimal delta-V trajectories designed by the patched conic method are optimized via the PSO method, and then the event dates and state variables of the spacecraft at these dates are obtained for designing the low-thrust trajectories. Secondly, the optimal control problem of designing the low-thrust trajectories is transformed into a boundary-valued problem. By the smooth technique and the proposed three step process, the low-thrust trajectories using multiple gravity assists can be solved efficiently. The effectiveness of the proposed methods is validated via numerical simulations.

Acknowledgments

This work is supported by the National Natural Science Foundation of China (NO. 11372150) and the National Basic Research Program of China (973 Program) (2012CB720000).

References

Armellin, R., Lizia, P.D., Toppeto, F., Lavagna, M., Bernelli-Zazzera, F., Berz, M., 2010. Gravity assist space pruning based on differential algebra. *Celest. Mech. Dyn. Astron.* 106 (1), 1–24.

¹ http://sophia.estec.esa.int/gtoc_portal/wp-content/uploads/2014/09/gtoc7_ranks.pdf [retrieved on 5 May 2015].

- Barucci, M.A., Cheng, A.F., Michel, P., et al., 2012. MarcoPolo-R near earth asteroid sample return mission. *Exp. Astron.* 33 (2–3), 645–684.
- Bertrand, R., Epenoy, R., 2002. New smoothing techniques for solving bang–bang optimal control problems—numerical results and statistical interpretation. *Optimal Control Appl. Meth.* 23 (4), 171–197.
- Caillau, J.B., Daoud, B., Gergaud, J., 2012. Minimum fuel control of the planar circular restricted three-body problem. *Celest. Mech. Dyn. Astron.* 114 (1–2), 137–150.
- Casalino, L., Colasurdo, G., Pastrone, D., 1999. Optimal low-thrust escape trajectories using gravity assist. *J. Guidance, Control, Dyn.* 22 (5), 637–642.
- Casalino, L., Colasurdo, G. March 2015. “Multi-spacecraft exploration of the asteroid belt”. In: Workshop of 7th edition of the Global Trajectory Optimisation Competition, Rome.
- Chen, Y., Baoyin, H., Li, J., 2014. Accessibility of main-belt asteroids via gravity assists. *J. Guidance, Control, Dyn.* 37 (2), 623–632.
- Dankanich, J.W., Landau, D., Martini, M.C., Oleson, S.R., Rivkin, A., 2010. Main Belt Asteroid Sample Return Mission Design. AIAA (No. 7015, pp. 1–17).
- Dunham, D.W., Farquhar, R.W., McAdams, J.V., Holdridge, M., Nelson, R., Whittenburg, K., Harch, A., 2002. Implementation of the first asteroid landing. *Icarus* 159 (2), 433–438.
- Gao, Y., 2012. Results and rankings of the 4th edition Chinese Space Trajectory Design Competition and the 6th Global Trajectory Optimization Competition. *Mech. Eng.* 34, 95–96 (in Chinese).
- Jiang, F., Baoyin, H., Li, J., 2012. Practical techniques for low-thrust trajectory optimization with homotopic approach. *J. Guidance, Control, Dyn.* 32 (1), 245–258.
- Jiang, F., Chen, Y., Liu, Y., Baoyin, H., Li, J., 2014. GTOC5: results from the Tsinghua university. *Acta Futura* 8, 37–44.
- Kawaguchi, J.I., Fujiwara, A., Uesugi, T., 2008. Hayabusa—its technology and science accomplishment summary and Hayabusa-2. *Acta Astronaut.* 62 (10), 639–647.
- Kennedy, J., 2010. Particle swarm optimization. In: *Encyclopedia of Machine Learning*. Springer, US, pp. 760–766.
- Kuninaka, H., Nishiyama, K., Funaki, I., Yamada, T., Shimizu, Y., Kawaguchi, J.I., 2007. Powered flight of electron cyclotron resonance ion engines on Hayabusa explorer. *J. Propul. Power* 23 (3), 544–551.
- Lau, C.O., Hulkower, N.D., 1987. Accessibility of near-earth asteroids. *J. Guidance, Control, Dyn.* 10 (3), 225–232.
- Lauretta, D.S., Team, O.R. March 2012. “An overview of the OSIRIS-REx asteroid sample return mission”. In: *Lunar and Planetary Institute Science Conference Abstracts*, vol. 43, No. 2491.
- Lin, Q., Loxton, R., Teo, K.L. 2014. “Optimal control of nonlinear switched systems: computational methods and applications”. *Journal of the Operations Research Society of China*.
- Loxton, R., Lin, Q., Teo, K.L. 2014. “Switching time optimization for nonlinear switched systems: direct optimization and the time-scaling transformation”. *Pacific Journal of Optimization*.
- McConaghy, T.T., Debban, T.J., Petropoulos, A.E., Longuski, J.M., 2003. Design and optimization of low-thrust trajectories with gravity assists. *J. Spacecr. Rockets* 40 (3), 380–387.
- Morbiddelli, A., Bottke, W.F., Froeschlé, C., Michel, P., 2002. Origin and evolution of near-Earth objects. *Asteroids III*, 409–422.
- Morimoto, M., Yamakawa, H., Yoshikawa, M., Abe, M., Yano, H., 2004. Trajectory design of multiple asteroid sample return missions. *Adv. Space Res.* 34 (11), 2281–2285.
- Olympio, J.T., 2011. Optimal control problem for low-thrust multiple asteroid tour missions. *J. Guidance, Control, Dyn.* 34 (6), 1709–1720.
- Pontani, M., Conway, B.A., 2010. Particle swarm optimization applied to space trajectories. *J. Guidance, Control, Dyn.* 33 (5), 1429–1441.
- Qiao, D., Cui, H., Cui, P., 2006. Evaluating accessibility of near-earth asteroids via earth gravity assists. *J. Guidance, Control, Dyn.* 29 (2), 502–505.
- Rao, A.V., 2009. A survey of numerical methods for optimal control. *Adv. Astron. Sci.* 135 (1), 497–528.
- Rasotto, M., Armellin, R., Lizia, P.D., Bernelli-Zazzera, F. 2013. “Optimal low-thrust transfers in two-body and three-body dynamics”. In: 64th International Astronautical Congress, Beijing.

- Russell, C.T., Capaccioni, F., Coradini, A., De Sanctis, M.C., Feldman, W.C., Jaumann, R., Zuber, M.T., 2007. “Dawn mission to Vesta and Ceres”. *Earth Moon Planet.* 101 (1–2), 65–91.
- Sears, D., Allen, C., Britt, D., Brownlee, D., Franzen, M., Gefert, L., Scott, E., 2004. “The Hera mission: multiple near-earth asteroid sample return”. *Adv. Space Res.* 34 (11), 2270–2275.
- Sims, J., Flanagan, S. January, 1997. “Preliminary design of low-thrust interplanetary missions.” NASA Technical Report, Document ID: 20000057422.
- Sims, J.A., Longuski, J.M., Staugler, A.J., 1997. V_8 leveraging for interplanetary missions: multiple-revolution orbit techniques. *J. Guidance, Control, Dyn.* 20 (3), 409–415.
- Strange, N.J., Longuski, J.M., 2002. Graphical method for gravity-assist trajectory design. *J. Spacecr. Rockets* 39 (1), 9–16.
- Tsuda, Y., Yoshikawa, M., Abe, M., Minamino, H., Nakazawa, S., 2013. System design of the Hayabusa 2-Asteroid sample return mission to 1999 JU3. *Acta Astron.* 91, 356–362.
- Woo, B., Coverstone, V.L., Cupples, M., 2006. Low-thrust trajectory optimization procedure for gravity-assist, outer-planet missions. *J. Spacecr. Rockets* 43 (1), 121–129.
- Yang, H., Baoyin, H., 2015. Fuel-optimal control for soft landing on an irregular asteroid. *IEEE T. Aero. Elec. Sys.* 51 (3).
- Zeng, X., Gong, S., Li, J., 2014. Fast solar sail rendezvous mission to near Earth asteroids. *Acta Astronaut.* 105 (1), 40–56.